Switchable and tunable film bulk acoustic resonator fabricated using barium strontium titanate active layer and Ta_2O_5/SiO_2 acoustic reflector

N. M. Sbrockey,[1,a)] T. S. Kalkur,[2] A. Mansour,[2] H. Khassaf,[3] H. Yu,[3] M. Aindow,[3] S. P. Alpay,[3] and G. S. Tompa[1]
[1]Structured Materials Industries, Inc., Piscataway, New Jersey 08854, USA
[2]Department of Electrical and Computer Engineering, Colorado State University at Colorado Springs, Colorado Springs, Colorado 80933, USA
[3]Department of Materials Science and Engineering and Institute of Materials Science, University of Connecticut, Storrs, Connecticut 06269, USA

(Received 2 June 2016; accepted 22 July 2016; published online 2 August 2016)

A solidly mounted acoustic resonator was fabricated using a $Ba_{0.60}Sr_{0.40}TiO_3$ (BST) film deposited by metal organic chemical vapor deposition. The device was acoustically isolated from the substrate using a Bragg reflector consisting of three pairs of Ta_2O_5/SiO_2 layers deposited by chemical solution deposition. Transmission electron microscopy verified that the Bragg reflector was not affected by the high temperatures and oxidizing conditions necessary to process high quality BST films. Electrical characterization of the resonator demonstrated a quality factor (Q) of 320 and an electromechanical coupling coefficient (K_t^2) of 7.0% at 11 V. *Published by AIP Publishing*. [http://dx.doi.org/10.1063/1.4960361]

Acoustic resonators are used in many applications, including timing standards in computers and industrial controllers and frequency standards in radio frequency (RF) devices such as filters and duplexers.[1,2] The active layer in commercial resonators is typically a thin film of piezoelectric material such as AlN or ZnO. Present technology acoustic resonators such as the film bulk acoustic resonator (FBAR) are passive devices, which are neither tunable nor switchable. Tunable and/or switchable resonators could significantly reduce cost and increase performance for RF products in communications, radar, and wireless data applications. Recently, there have been demonstrations of voltage induced acoustic resonance in thin films of perovskite materials which are not inherently piezoelectric, such as $SrTiO_3$[3–5] and $Ba_xSr_{1-x}TiO_3$ (BST).[6–11] These studies demonstrate the potential to develop acoustic resonators which can be switched or frequency tuned using a DC voltage control signal. In order to be practical, these devices must be efficient, capable of a wide tuning range, result in minimal insertion loss, and operate at low control voltages.

Previous works to develop voltage controlled acoustic resonators have used perovskite films deposited by pulsed laser deposition (PLD),[6,10] sputtering,[3,4,8,11] or chemical solution deposition (CSD).[12,13] Metal organic chemical vapor deposition (MOCVD) has the potential to produce higher quality oxide films than either sputtering or PLD, since no energetic ions are involved in the deposition process. Furthermore, MOCVD is economical and provides a simple and quantitative means for compositional grading,[14] which can improve the dielectric properties for complex oxide films. The tunability and coupling efficiency of the resonator should improve with higher quality films, since high quality films improve coupling efficiency and enable higher control voltage.[15] The only other published demonstration of a voltage induced acoustic resonator fabricated using an MOCVD deposited film was our work using $SrTiO_3$ (STO).[5] The electromechanical coupling efficiency of BST should be significantly higher than that for STO, as predicted through computational modeling,[16,17] and verified experimentally.[6–11] We note that BST is a leading material system for dielectrically tunable devices because of its high tunability near the ferroelectric phase transformation temperature T_C which can be tailored by adjusting its composition and internal strains.[18–21] For example, the T_C of bulk BST 60/40 ($Ba_{0.60}Sr_{0.40}TiO_3$) is just below room temperature (5 °C). Therefore, BST film compositions near $Ba_{0.60}Sr_{0.40}TiO_3$ are expected to be paraelectric at room temperature. BST films with significantly higher barium content are expected to be ferroelectric at room temperature. Acoustic resonators fabricated with ferroelectric BST films would exhibit undesirable hysteresis in resonator performance versus applied voltage. The intention of this work is to demonstrate a voltage controlled acoustic resonator based on MOCVD deposited paraelectric BST film, in order to improve the efficiency and commercial viability of voltage controlled resonators for RF device applications.

Solidly mounted resonator (SMR) structures were fabricated on both *c*-axis sapphire (α-Al_2O_3) and high resistivity silicon substrate. An acoustic Bragg reflector was first fabricated on the substrate, to acoustically isolate the resonator from the substrate. Since high temperatures are required for processing of high quality BST films, a Bragg reflector based on Pt/SiO_2[4,22] or Au/SiO_2[10,15] could not be used. Instead, a Bragg reflector was developed based on three pairs of alternating Ta_2O_5/SiO_2 films deposited by chemical solution deposition (CSD). The nominal thickness of the individual Ta_2O_5 and SiO_2 layers was a quarter wavelength of the device design frequency of 6.0 MHz. The platinum film of thickness 100 nm with a 20 nm titanium film adhesion layer was deposited on

[a)]Author to whom correspondence should be addressed. Electronic mail: sbrockey@structuredmaterials.com

0003-6951/2016/109(5)/052902/4/$30.00

top of the Bragg reflector by DC magnetron sputtering as the resonator bottom electrode. The bottom electrode was patterned using standard photolithography and ion milling. The BST film of composition $Ba_{0.60}Sr_{0.40}TiO_3$ was deposited by MOCVD at a substrate temperature of 650 °C. The BST film was deposited in two stages, with atmospheric exposure in between. The total target thickness of the BST film was 140 nm. This two stage deposition process is intended to minimize film defects which could cause electrical shorts or leakage current in the film. After the second BST film deposition, the device was annealed at 800 °C in an oxidizing environment. The device top electrode was then applied using 100 nm of Pt film deposited by DC magnetron sputtering and patterning by photolithography and ion milling.

To verify the device structure, transmission electron microscopy (TEM) specimens were prepared of a similar device fabricated on a high resistivity silicon substrate. The TEM specimens were prepared using an FEI Strata 400S dual-beam focused ion beam (FIB) instrument, which is equipped with a flip-stage and a scanning transmission electron microscopy (STEM) detector for improved final thinning. A 3 μm Pt layer was deposited *in-situ* on to the resonator TEM specimen to protect the surface during ion milling. The deposition was performed in two steps: the first 1 μm of Pt was deposited using the electron beam to crack the organometallic Pt precursor, and the remaining 2 μm of Pt was deposited using the ion beam. The ion column accelerating voltage was 30 kV throughout the milling process. The ion beam currents were reduced iteratively to a value of 9.7 pA during final milling to avoid excessive Ga^+ implantation and beam damage. The FIB-cut slices were mounted onto Mo Omni grids and attached at two corners to limit mechanical buckling of the specimens during final thinning. The FIB-cut slices were examined in a FEI Tecnai T12 TEM operated at an accelerating voltage of 120 kV and equipped with an EDAX ultra-thin window energy-dispersive X-ray spectroscopy (EDXS) system.

Figure 1(a) shows a bright field TEM image of an FIB-cut section through the acoustic resonator structure. The thickness of each layer in the device was measured from the image directly, and the character of the material was verified using EDXS analysis. These data show that the structure comprises a 134 nm thick Pt top electrode, a 142 nm thick, dense, uniform, poly-crystalline BST layer, a 126 nm thick Pt layer under the BST, a 26 nm Ti adhesion layer, and the six layer Bragg reflector consisting of three pairs of 267 nm thick SiO_2 and 137 nm thick Ta_2O_5 layers. The TEM micrograph clearly shows that even after high temperature processing of the BST films, the Bragg reflector stack is still well defined with sharp interfaces and all layer thicknesses at their target values. Figure 1(b) shows a top view optical micrograph of the finished acoustic resonator device with ground-signal-ground electrodes. The active area of the resonator is the 10 μm $\times$ 10 μm square defined by the overlap of the upper and lower electrodes.

RF characterization of the resonator was performed using an Agilent vector network analyzer with Cascade Microtech ground-signal-ground microprobes. The return loss (S_{11}) of the resonator was determined after calibrating the measurement set up with on-wafer open circuit and short circuit calibration structures. Figure 2 shows the variation of return loss with frequency for various bias voltages. With no bias voltage applied, no resonance is observed and the device acts as a simple capacitor. As the bias voltage is increased, S_{11} shows a characteristic resonance with increasing notch depth and decreasing resonant frequency. The resonant frequency decreases from 6.816 GHz at 1 V to 6.767 GHz at 11 V, representing a tunability of about 0.8% over this voltage range. The maximum return loss was 16.3 dB at an applied bias of 11 V. Figure 3 shows the variation of the real part of the resonator impedance with frequency for various bias voltages. The impedance of the resonator increases from 12 Ω to 37 Ω with the application of a 11 V bias voltage, which confirms voltage induced piezoelectricity in the MOCVD deposited BST film.

The variation of the series and parallel resonance frequencies with applied bias is shown in Figure 4. The series resonance frequency decreases approximately linearly with applied bias from 4 V to 11 V, representing a series resonance frequency tunability of about −0.9%. There is a slight increase in the series resonance frequency with applied bias from 1 V to 4 V resulting in a positive tunability at these low control voltages. Similar results were reported for an acoustic resonator fabricated using sputter deposited BST film[11] and

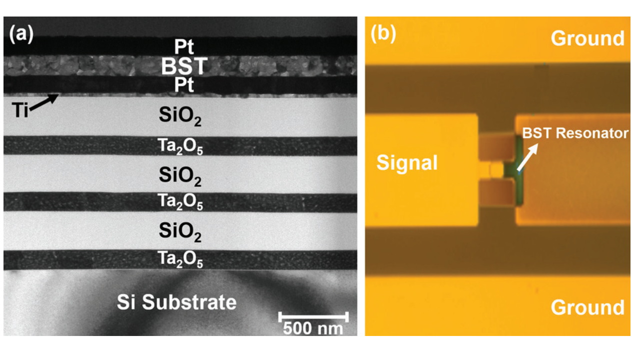

FIG. 1. Solidly mounted acoustic resonator fabricated with MOCVD deposited BST film and MOSD deposited SiO_2/Ta_2O_5 Bragg reflector: (a) Cross sectional TEM image of the device fabricated on a high resistivity silicon substrate; (b) Planar view optical micrograph.

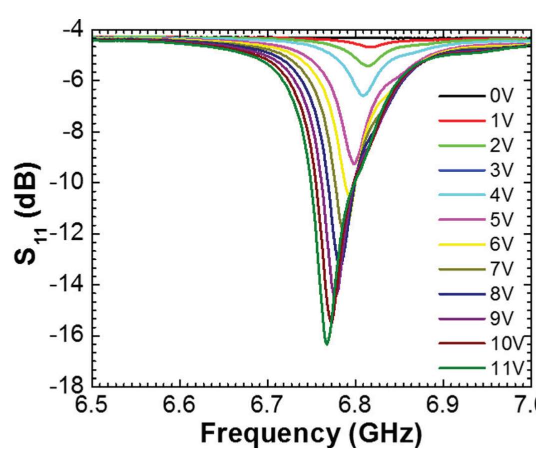

FIG. 2. Measured return loss (S_{11}) with frequency for the solidly mounted resonator under various bias voltages.

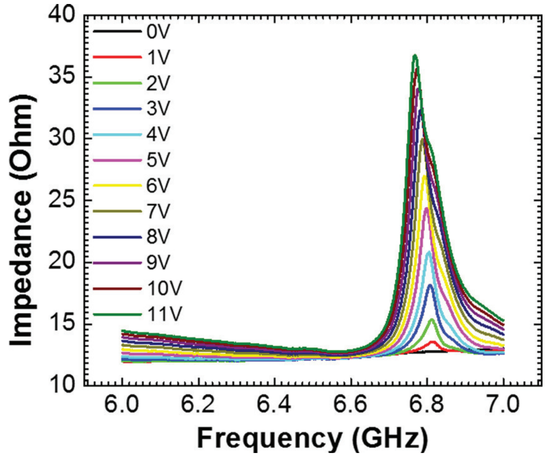

FIG. 3. Measured input impedance (real part magnitude) as a function of frequency for the solidly mounted resonator.

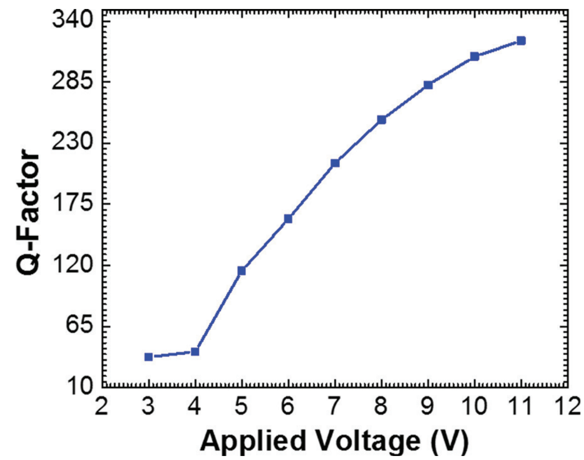

FIG. 5. Calculated value of the quality factor (Q) for the solidly mounted resonator as a function of applied bias voltage.

attributed to the non-linear variation of the electromechanical coupling coefficient and the elastic constants with applied bias. The parallel resonance frequency decreases slightly as the bias voltage increases from 1 V to 11 V, which may be due to the increase in BST thickness due to the electrostriction effect of the applied bias voltage. The abrupt increase in parallel resonance frequency at 6 V may be attributed to an electrostriction induced phase transition of the BST thin film.[20]

Figure 5 shows the variation of the quality factor (Q) of the resonator with the applied bias voltage. The quality factor is calculated using the following expression:

$$Q = \left(\frac{f}{2}\right)\left(\frac{\delta\Phi}{\delta f}\right)\Big|_{f=f_{res}}, \tag{1}$$

where Φ is the phase and f is the resonance frequency. The quality factor was found to increase with increasing bias voltage above 4 V, as shown in Figure 5. A quality factor of 320 was observed at a bias voltage of 11 V. The electromechanical coupling coefficient of the resonator is calculated using the following expression:

$$K_t^2 = \left(\frac{\pi}{2}\right)\left(\frac{f_s}{f_p}\right)\tan\left[\frac{\pi}{2}\left(\frac{f_p - f_s}{f_p}\right)\right], \tag{2}$$

where f_s and f_p are the series and parallel resonance frequencies, respectively. The electromechanical coupling coefficient does not change significantly with applied voltage from 1 V to 6 V, as shown in Figure 6. Increasing the bias above 6 V increases the electromechanical coefficient to a maximum observed value of 7.69% at 8 V.

The observed values for K_t^2 are comparable to those for commercially available AlN based resonators, which are not tunable or switchable. Of the published studies for voltage controlled acoustic resonators, only one study reported a higher K_t^2 value of 8.09% at a bias voltage of 60 V.[11] The use of the MOCVD deposited BST film is shown to result in high efficiency acoustic resonators, as evidenced by the high values of Q and K_t^2 observed in this work. The use of the CSD deposited Ta_2O_5/SiO_2 Bragg reflector enables the high process temperatures and oxidizing conditions, which are necessary to produce high quality BST films. Also significant is the fact that the device demonstrated in this work operated at low control voltages, of 11 V or less. Low voltage

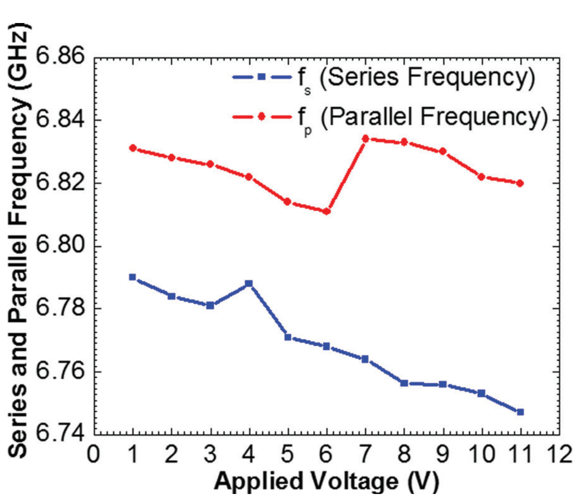

FIG. 4. Measured series resonance frequency (f_s) and parallel resonance frequency (f_p) as a function of applied bias voltage.

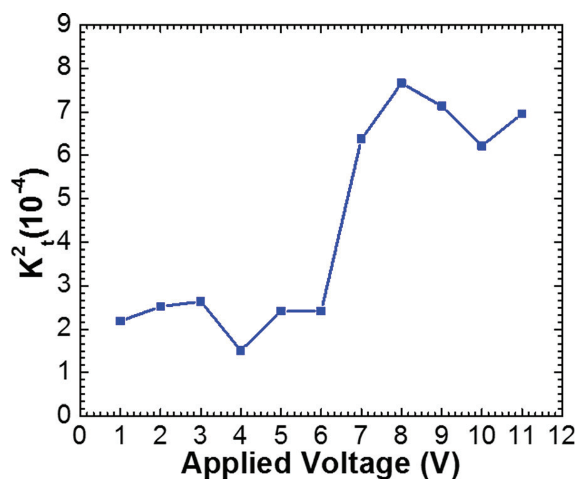

FIG. 6. Calculated value of the Electromechanical Coupling Coefficient (K_t^2) for the solidly mounted resonator as a function of applied bias voltage.

operation and high efficiency are key performance parameters for practical implementation of voltage controlled acoustic resonators in RF products.

The authors gratefully acknowledge financial support through STTR Phase II Contract No. W911NF-13-C-0029 from the U.S. Army Research Office.

[1]S. V. Krishnaswamy, J. Rosenbaum, S. Horwitz, C. Vale, and R. A. Moore, "Film bulk acoustic wave resonator technology," in *Proceedings of the 1990 IEEE Ultrasonics Symposium* (IEEE, 1990), pp. 529–536.
[2]F. Z. Bi and B. P. Barber, "Bulk acoustic wave RF technology," IEEE Microwave Mag. **9**(5), 65–80 (2008).
[3]K. Morito, Y. Iwazaki, T. Suzuki, and M. Fujimoto, J. Appl. Phys. **94**, 5199 (2003).
[4]G. N. Saddik, D. S. Boesch, S. Stemmer, and R. A. York, Appl. Phys. Lett. **91**, 043501 (2007).
[5]N. M. Sbrockey, G. S. Tompa, T. S. Kalkur, J. Zhang, S. P. Alpay, and M. W. Cole, J. Vac. Sci. Technol., B **30**(6), 061202 (2012).
[6]X. Zhu, J. D. Phillips, and A. Mortazawi, in *IEEE/MTT-S International Microwave Symposium* (2007), p. 671.
[7]S. Tappe, U. Böttger, and R. Waser, Appl. Phys. Lett. **85**, 624 (2004).
[8]G. N. Saddik and R. A. York, in *IEEE/MTT-S International Microwave Symposium* (2011), p. 1.
[9]V. M. Mukhortov, S. V. Biryukov, Y. I. Golovko, G. Y. Karapet'yan, S. I. Masychev, and V. M. Mukhortov, Tech. Phys. Lett. **37**, 207 (2011).
[10]J. Berge, A. Vorobiev, W. Steichen, and S. Gevorgian, IEEE Microwave Wireless Compon. Lett. **17**, 655 (2007).
[11]T.-Y. Yang, S.-W. Jiang, R.-G. Li, and B. Jiang, Chin. Phys. B **21**(10), 106801 (2012).
[12]T. S. Kalkur, N. Sbrockey, and G. S. Tompa, "MOD deposited BST film based thin tunable film bulk acoustic resonator (TFBAR)," e-J. Surf. Sci. Nanotechnol. **10**, 558–560 (2012).
[13]R. C. Toonen and M. W. Cole, "Third-order electric-field-induced dipolar resonances from patterned barium-strontium-titanate thin-films," Appl. Phys. Lett. **100**(22), 222908 (2012).
[14]N. M. Sbrockey, M. W. Cole, T. S. Kalkur, M. Luong, J. E. Spanier, and G. S. Tompa, Integr. Ferroelectr. **126**, 21 (2011).
[15]J. Berge, M. Norling, A. Vorobiev, and S. Gevorgian, "Field and temperature dependent parameters of the dc field induced resonances in $Ba_xSr_{1-x}TiO_3$-based tunable thin film bulk acoustic resonators," J. Appl. Phys. **103**(6), 064508 (2008).
[16]A. Noeth, T. Yamada, A. K. Tagantsev, and N. Setter, J. Appl. Phys. **104**, 094102 (2008).
[17]F.-C. Sun, H. Khassaf, and S. P. Alpay, J. Mater. Sci. **49**(17), 5978–5985 (2014).
[18]P. Bao, T. J. Jackson, X. Wang, and M. J. Lancaster, J. Phys. D: Appl. Phys. **41**(6), 063001 (2008).
[19]T. Yamada, O. Vladimir, A. N. Sherman, P. Muralt, A. K. Tagantsev, and N. Setter, Appl. Phys. Lett. **89**(3), 032905 (2006).
[20]H. Khassaf, N. Khakpash, F. Sun, N. M. Sbrockey, G. S. Tompa, T. S. Kalkur, and S. P. Alpay, Appl. Phys. Lett. **104**, 202902 (2014).
[21]G. Subramanyam, M. W. Cole, N. X. Sun, T. S. Kalkur, N. M. Sbrockey, G. S. Tompa, X. Guo, C. L. Chen, S. P. Alpay, G. A. Rossetti, Jr., K. Dayal, L. Q. Chen, and D. G. Schlom, "Challenges and opportunities for multi-functional oxide thin films for voltage tunable RF/microwave components," J. Appl. Phys. **114**, 191301 (2013).
[22]G. N. Saddik, J. Son, S. Stemmer, and R. A. York, J. Appl. Phys. **109**(9), 091606 (2011).